Journal of Biomolecular NMR, **14:** 133–140, 1999.
KLUWER/ESCOM

Gradient and sensitivity enhanced multiple-quantum coherence in heteronuclear multidimensional NMR experiments

Xiang Ming Kong, Kong Hung Sze & Guang Zhu*
Department of Biochemistry, Hong Kong University of Science and Technology, Clear Water Bay, Kowloon, Hong Kong, China

Received 9 December 1998; Accepted 12 March 1999

Key words: HMQC, multidimensional NMR, protein, sensitivity enhancement

Abstract

Recent studies have indicated that the relaxation rate of the ^{1}H-^{13}C multiple-quantum coherence is much slower than that of the ^{1}H-^{13}C single-quantum coherence for non-aromatic methine sites in ^{13}C labeled proteins and in nucleic acids at the slow tumbling limit. Several heteronuclear experiments have been designed to use a multiple-quantum coherence transfer scheme instead of the single-quantum transfer method, thereby increasing the sensitivity and resolution of the spectra. Here, we report a constant time, gradient and sensitivity enhanced HMQC experiment (CT-g/s-HMQC) and demonstrate that it has a significant sensitivity enhancement over constant time HMQC and constant time gradient and sensitivity enhanced HSQC experiments (CT-g/s-HSQC) when applied to a ^{13}C and ^{15}N labeled calmodulin sample in D_2O. We also apply this approach to 3D NOESY-HMQC and doubly sensitivity enhanced TOCSY-HMQC experiments, and demonstrate that they are more sensitive than their HSQC counterparts.

Introduction

It is known that the large one-bond ^{13}C-^{1}H dipolar interaction and geminal ^{1}H-^{1}H homonuclear dipolar interaction are the major sources of relaxation for transverse ^{1}H and ^{13}C magnetization in ^{13}C labeled macrobiomolecules (Griffey and Redfield, 1987; Grzesiek et al., 1995). The contribution to the relaxation of non-aromatic methine systems from chemical shift anisotropy (CSA) is negligible, even in a high magnetic field, due to its small value (Palmer et al., 1992). To a first order approximation, the relaxation of ^{13}C-^{1}H multiple-quantum coherence is not affected by the ^{13}C-^{1}H dipolar interaction for a molecule at the slow tumbling limit (Griffey and Redfield, 1987). Therefore, the relaxation rate of ^{13}C-^{1}H multiple-quantum coherence for the methine sites is slower than that of ^{1}H and ^{13}C single-quantum coherence. This property has found many applications in heteronuclear multidimensional NMR experiments (Grzesiek et al., 1995; Grzesiek and Bax, 1995; Marino et al., 1997; Shang et al., 1997; Swapna et al., 1997). In these applications, the HMQC experiment offers much better sensitivity than the HSQC experiment, and this result is in good agreement with theoretical calculations (Grzesiek and Bax, 1995; Marino et al., 1997).

It has been demonstrated that the conventional HSQC experiment can be greatly improved by employing a sensitivity enhancement scheme (Palmer et al., 1991; Kay et al., 1992; Schleucher et al., 1994). The sensitivity enhancement is achieved by retaining both the x- and y-components of the indirectly detected dimensions by a process which is called either Preservation of Equivalent Pathways (PEP) (Cavanagh and Rance, 1993) or Coherence Order Selective-Coherence Transfer (COS-CT) (Sattler et al., 1995). This basic sensitivity enhancement scheme has been widely used (Schleucher et al., 1993; Muhandiram and Kay, 1994; Yamazaki et al., 1994). We have recently reported a gradient and sensitivity enhanced HMQC experiment (g/s-HMQC) using a similar approach and

*To whom correspondence should be addressed. E-mail: gzhu@ust.hk

shown that, for an IS spin system, a sensitivity enhancement by a factor of $\sqrt{2}$ over the conventional HMQC experiment can be achieved (Zhu et al., 1998). Here, we propose a constant-time, gradient and sensitivity enhanced HMQC (CT-g/s-HMQC) experiment, with a spin lock being used to remove homonuclear coupling effects. We demonstrate that the sensitivity of this CT-g/s-HMQC experiment shows a significant improvement over both the CT-HMQC experiment and its HSQC counterpart (CT-g/s-HSQC) for the ^{13}C-^{1}H moiety. This experiment will be particularly useful for protein NMR studies using ^{13}C-^{1}H correlation, as all the amino acids except glycine have α carbons which are methine moieties. The use of the PEP/COS-CT approach allows a sensitivity enhancement up to a factor of 1.36 for experiments correlating ^{13}C and ^{1}H as discussed below. We have also applied this basic pulse sequence to 3D NOESY-HMQC and doubly sensitivity enhanced 3D TOCSY-HMQC experiments, and demonstrated that they are more sensitive than their HSQC counterparts. However, it should be noted that experiments which include a TOCSY mixing scheme are seldomly applied to large ^{13}C labeled proteins due to the effect of the ^{13}C-^{1}H dipolar coupling on T_2 of ^{13}C attached protons (Bax, A., personal communication).

Methods

Figure 1A shows the pulse sequence of the constant time, gradient and sensitivity enhanced HMQC experiment (CT-g/s-HMQC) with a spin-lock field. A brief description of the magnetization transfer is given below. After the constant time t_1 evolution, the magnetization is:

$$M_a = I_x(S_y \cos\omega_S t_1 + S_x \sin\omega_S t_1)\cos\pi J_{CC} T$$

where J_{CC} is the aliphatic carbon homonuclear J coupling constant and T is the constant time for the t_1 evolution period ($T = 1/J_{CC}$). The spin-lock field locks I magnetization on the x-axis. After two $2\Delta(= 1/2J_{CH})$ delays to transfer back the magnetization, the magnetization before acquisition is:

$$M_b = \begin{cases} \left(\frac{1}{2}\right)[I^+ \exp(i\omega_s t_1 - i\theta_i + i\theta_2) \\ \quad + I^- \exp(-i\omega_s t_1 + i\theta_i - i\theta_2)], & \phi 2 = x \\ \left(\frac{1}{2}\right)[I^+ \exp(-i\omega_s t_1 + i\theta_i + i\theta_2) \\ \quad - I^- \exp(i\omega_s t_1 - i\theta_i - i\theta_2)], & \phi 2 = -x \end{cases}$$

where $\theta_1 = \gamma_C B_1(z)\tau_1$ and $\theta_2 = \gamma_H B_2(z)\tau_2$ with $B_i(z)$ and τ_i being the strength and duration of the gradients G1 and G2, respectively. Therefore, by proper arrangement of the $\phi 2$ phase and the gradient settings, no signal loss will occur. The final pure absorption spectrum can be obtained by data processing as described previously (Kay et al., 1992; Zhu et al., 1998). In the discussion above, we have assumed that the x- and y-components of magnetization have the same amplitude before acquisition, even though they experience different magnetization transfer pathways. However, in reality, there is a difference between them caused by their different relaxation processes and, especially relevant to our experiment, a different homonuclear coupling effect. Thus, the magnetization M_b without gradients should be expressed as follows

$$M_b = \begin{cases} I\cos\omega_s t_1 + (1-B) I_y \sin\omega_s t_1, & \phi 2 = x \\ -I\cos\omega_s t_1 + (1-B) I_y \sin\omega_s t_1, & \phi 2 = -x \end{cases}$$

$$= \begin{cases} \frac{(2-B)}{2}(I_x \cos\omega_s t_1 + I_y \sin\omega_s t_1) \\ \quad -\frac{B}{2}(-I_x \cos\omega_s t_1 + I_y \sin\omega_s t_1), & \phi 2 = x \\ \frac{(2-B)}{2}(-I_x \cos\omega_s t_1 + I_y \sin\omega_s t_1) \\ \quad -\frac{B}{2}(I_x \cos\omega_s t_1 + I_y \sin\omega_s t_1), & \phi 2 = -x \end{cases}$$

where B is an imbalance factor between magnetizations I_x and I_y. From the above expressions, we can see that the gradients serve to select the balanced part and to dephase the imbalance part of the I_x and I_y magnetizations. Any imbalance will lead to a reduced gain in sensitivity. Without the gradients, data processing as stated above would result in quadrature image artifacts. Overall, the gradient and sensitivity enhancement process can be summarized as:

$$I_x(S_y \cos\omega_s t_1 + S_x \sin\omega_s t_1) \overset{PEP/COS-CT}{\longrightarrow} \begin{cases} \frac{(2-B)}{2}(I_x \cos\omega_s t_1 + I_y \sin\omega_s t_1), & \phi 2 = x \\ \frac{(2-B)}{2}(-I_x \cos\omega_s t_1 + I_y \sin\omega_s t_1), & \phi 2 = -x \end{cases}$$

In the PEP/COS-CT process, one component of the magnetization must experience an additional 2Δ delay in the multiple-quantum coherence state. During this additional delay, the magnitude of this component will be reduced due to $C_\alpha - C_\beta$ coupling. If the difference in the relaxation rates of the x- and y- components during the PEP/COS-CT is negligible, then the remaining factor 1−B is

$$1 - B = \cos(2\pi J_{CC}\Delta) = 0.92,$$

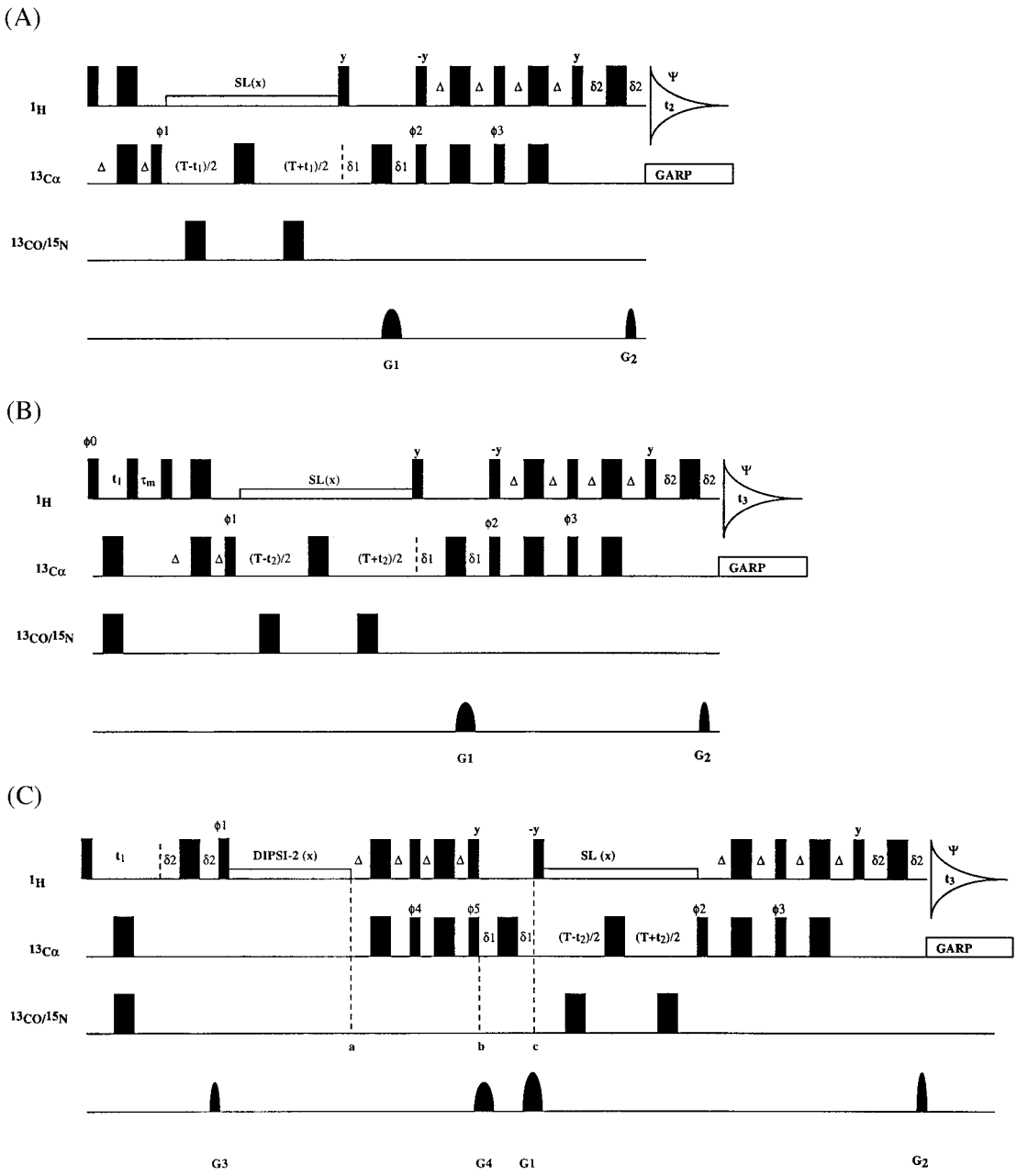

Figure 1. (A) Pulse sequence of the 2D constant time, gradient and sensitivity enhanced HMQC experiment (CT-g/s-HMQC). The thin and thick vertical bars represent 90° and 180° pulses, respectively. Unlabeled pulses are applied along the x-axis. Two transients are recorded for each t_1 value. The first transient is acquired by using the phase cycle $\phi1 = 0, 0, 2, 2$; $\phi2 = 0, 2$; $\phi3 = 1, 3$; Rec. $\Psi = 0, 2, 2, 0$ and the gradient setting is G1 = G2. For the second transient, the signs of the phase $\phi2$ and the gradient G2 are changed. A pure absorption spectrum can be obtained as stated in the text. (B) Pulse sequence of the 3D g/s-NOESY-HMQC experiment. The phase cycle used is $\phi0 = 0, 0, 0, 0, 2, 2, 2, 2$; $\phi1 = 0, 0, 2, 2$; $\phi2 = 0, 2$; $\phi3 = 1, 3$; Rec. $\Psi = 0, 2, 2, 0, 2, 0, 0, 2$ and the gradient setting is G1 = G2. Quadrature detection in the F1 dimension is obtained via the States-TPPI method by increasing the phases of $\phi0$. Absorption mode in the F2 dimensions is obtained as stated in the text for the CT-g/s-HMQC experiment. (C) Pulse sequence of the 3D doubly sensitivity enhanced TOCSY-HMQC experiment. The phase cycle is $\phi1 = 1$; $\phi2 = 0, 2$; $\phi3 = 1, 3$; $\phi4 = 0$; $\phi5 = 1$; Rec. $\Psi = 0, 2$ and the gradient settings are G1 = G2, and G3 = G4. Absorption-mode spectra in the F1 and F2 dimensions are obtained as discussed in the text. In these pulse sequences, the soft C_α pulses, with the carrier frequency at 58 ppm, are applied with a power of $\gamma B = 10$ kHz to leave a null excitation in the carbonyl region. The 180° carbonyl pulse is a SINC shaped pulse (Hyre and Spicer, 1995) of 256 μs duration with a phase ramp (Patt, 1992) to shift the excitation region to the carbonyl carbons. Proton spin lock is achieved by using a power of 5 kHz with the carrier at 4.3 ppm in the center of the H_α region. Pulsed field gradients are applied along the z-axis. The magnitudes of the gradients G1, G2, G3 and G4 are 20, 20, 10 and 10 G/cm with durations of 0.8, 0.2, 0.2 and 0.8 ms, respectively. The constant time T is set to 27.2 ms. The delays Δ, δ1 and δ2 are set to $1/4J = 1.6$ ms, 0.9 ms and 0.4 ms, respectively.

with $J_{CC} = 40$ Hz and $2\Delta = 3.2$ ms being used. Since the pulsed field gradient will remove the imbalance between the magnitudes of the magnetization components I_x and I_y, the magnitude of the final detectable signal would be (2−B)/2, that is 0.96. Thus, the maximum sensitivity enhancement of the CT-g/s-HMQC experiment when compared with the conventional experiment would be $0.96\sqrt{2} = 1.36$.

During the constant time t_1 evolution period, proton homonuclear coupling would significantly lower the sensitivity of the experiment if it was to occur. Consequently, we have included a spin-lock sequence to remove this coupling. This spin lock serves to lock the proton magnetization on the x-axis with minimal magnetization loss caused by the offset effect and TOCSY type magnetization transfer from H_α to H_β, H_γ and so on. A relatively strong CW (5–7 kHz) spin-lock field is preferred (Grzesiek and Bax, 1995). An alternative would be to substitute the constant time $^{13}C_\alpha$ evolution period with a spin lock by the simultaneous-CT method (Shang et al., 1997; Swapna et al., 1997). However, the digital resolution of the ^{13}C dimension would then be lower. Selective 180° ^1H pulses could be also employed to remove homonuclear couplings, as has been demonstrated for nucleic acids (Zhu et al., 1994). However, they are less suitable for proteins as the chemical shifts of the C_α and C_β protons may overlap.

In practice, the theoretical sensitivity enhancement by PEP/COS-CT may not be achieved due to signal loss caused by the larger number of pulses, delays to insert gradients and the additional 2Δ delay to transfer back the x- and y-components of the magnetization. If we assume that the longitudinal relaxation time is much longer than the delay, 2Δ, then the PEP/COS-CT approach of sensitivity enhancement is only applicable when

$$(1 + (1 - B)e^{-2\Delta R_{MQ}})e^{-2R_c\delta_1 - 2R_H\delta_2} > \sqrt{2}$$

where R_{MQ} is the relaxation rate of multiple-quantum coherence; R_C and R_H are the transverse relaxation rates of the single-quantum coherence of carbon and proton, respectively. According to the model of Grzesiek and Bax (1995b), and assuming isotropic tumbling, a theoretical enhancement of 15% could be achieved for a protein of 20 kDa with a τ_c of 8 ns, and for a protein of 40 kDa, no enhancement by the PEP/COS-CT approach would be obtained. Though the ^{13}C-^1H multiple-quantum coherence relaxation is not affected by the ^{13}C-^1H dipole-dipole interaction at the slow tumbling limit, the T_2 relaxation caused by the ^1H-^1H dipole-dipole interaction between neighboring protons can be significant and depends on the local proton density. It could be expected that random fractional deuteration of proteins can be used to reduce the ^1H-^1H dipole-dipole induced relaxation effect (Torchia et al., 1988; Reisman et al., 1991; Nietlispach et al., 1996), and to extend the protein size limit for the application of the CT-g/s-HMQC experiment.

Figures 1B and 1C depict the pulse schemes of the gradient and sensitivity enhanced 3D NOESY-HMQC (g/s-NOESY-HMQC) and the doubly sensitivity enhanced 3D TOCSY-HMQC experiments, respectively. The 3D g/s-NOESY-HMQC experiment is a straightforward extension of the CT-g/s-HMQC experiment and uses the same data processing procedure to produce the absorption spectrum in the F2 dimension. The double sensitivity enhancement of the TOCSY-HMQC experiment is achieved by retaining the x- and y-components of the evolving magnetization in the F1 and F2 dimensions. The TOCSY mixing is achieved by the DIPSI-2 sequence (Shaka et al., 1988) which is isotropic for homonuclear magnetization transfer in the x-, y- and z-directions. For each set of t_1 and t_2 values, four transients with different $\phi1$ and $\phi2$ phases and different combinations of gradients are acquired and stored separately. The two sets of gradients (G3 and G4) and (G1 and G2) select the magnetization transfer from $^1H_\alpha$ to $^{13}C_\alpha$ and from $^{13}C_\alpha$ back to $^1H_\alpha$, respectively, and also dephase any imbalance between the magnetizations along the x- and y-axes during the PEP/COS-CT process. Following the standard product operator analysis (Sørensen et al., 1983; Ernst et al., 1987), a brief description of magnetization transfer can be given as

$$\sigma_a = I_y \cos(\omega_I t_1 + \theta_3) \mp I_z \sin(\omega_I t_1 + \theta_3) \qquad (\phi1 = 1, 3)$$

$$\sigma_b = 2I_z[S_y \cos(\omega_I t_1 + \theta_3) \mp S_x \sin(\omega_I t_1 + \theta_3)] \qquad (\phi1 = 1, 3)$$

$$\sigma_c = -2I_z[S_y \cos(\omega_I t_1 + \theta_3 \mp \theta_4 + \theta_1) \pm S_x \sin(\omega_I t_1 + \theta_3 \mp \theta_4 + \theta_1)] \qquad (\phi1 = 1, 3)$$

where θ_1 is defined as before, $\theta_3 = \gamma_H B_3(z)\tau_3$ and $\theta_4 = \gamma_C B_4(z)\tau_4$. The 90° ^1H pulse before time point *b* serves to transfer the multiple-quantum coherence

to single-quantum, so that the magnetization encoded by gradient G3 can be decoded by gradient G4 and encoded again by gradient G1. The 90° ^{1}H pulse after time point *c* then transfers the single-quantum coherence back to multiple-quantum coherence to exploit its better relaxation properties for the evolution of the carbon signal. The magnetization transfer during the period from *a* to *b* is a reverse HSQC or HMQC sensitivity enhancement approach. Taking account of the phases of the signals (Levitt, 1997), the magnitudes of the four transients before acquisition are:

$$\sigma_1 = (\frac{2-B}{2})^2(i\cos\omega_I t_1 + \sin\omega_I t_1)(i\sin\omega_S t_2 + \cos\omega_S t_2)$$
$$(\phi 1 = y, \phi 2 = x, G1 = G2, G3 = G4)$$
$$\sigma_2 = (\frac{2-B}{2})^2(i\cos\omega_I t_1 + \sin\omega_I t_1)(i\sin\omega_S t_2 - \cos\omega_S t_2)$$
$$(\phi 1 = y, \phi 2 = -x, G1 = -G2, G3 = G4)$$
$$\sigma_3 = (\frac{2-B}{2})^2(i\cos\omega_I t_1 - \sin\omega_I t_1)(i\sin\omega_S t_2 + \cos\omega_S t_2)$$
$$(\phi 1 = -y, \phi 2 = x, G1 = G2, G3 = -G4)$$
$$\sigma_4 = (\frac{2-B}{2})^2(i\cos\omega_I t_1 - \sin\omega_I t_1)(i\sin\omega_S t_2 - \cos\omega_S t_2)$$
$$(\phi 1 = -y, \phi 2 = -x, G1 = -G2, G3 = -G4)$$

Proper combination of these four transients leads to:

$$\begin{aligned} M_1 &= \sigma_1 + \sigma_2 + \sigma_3 + \sigma_4 \\ &= -(2-B)^2\cos\omega_I t_1 \sin\omega_S t_2 \\ M_2 &= \sigma_1 + \sigma_2 - \sigma_3 - \sigma_4 \\ &= (2-B)^2 i \sin\omega_I t_1 \sin\omega_S t_2 \\ M_3 &= \sigma_1 - \sigma_2 + \sigma_3 - \sigma_4 \\ &= (2-B)^2 i \cos\omega_I t_1 \cos\omega_S t_2 \\ M_4 &= \sigma_1 - \sigma_2 - \sigma_3 + \sigma_4 \\ &= (2-B)^2 \sin\omega_I t_1 \cos\omega_S t_2 \end{aligned}$$

These four FIDs can be used to construct a pure absorption 3D TOCSY-HMQC spectrum, using Fourier transformation, after applying a 90° phase shift to M_2 and M_3, and changing the sign of M_4. The theoretical sensitivity enhancement of this 3D TOCSY-HMQC experiment over its conventional version can be $(1.36)^2$ if relaxation loss during the two additional 2Δ delays is negligible.

Results and discussion

To demonstrate the advantage of the proposed gradient and sensitivity enhanced HMQC pulse sequence, experiments were performed on a ^{13}C and ^{15}N labeled calmodulin sample in D_2O, at pH = 6.0 and a temperature of 27 °C using a Varian Inova 500 MHz spectrometer. Figures 2A–C show small regions taken from constant time g/s-HSQC, constant time HMQC (Ikura et al., 1991; Tjandra et al., 1995; Marino et al., 1997), and constant time g/s-HMQC 2D spectra, respectively. Figure 2D shows 1D cross-sections from Figures 2A–C, taken at ^{13}C = 65.1 ppm. It can be seen from the spectra that the proposed constant time g/s-HMQC experiment with spin lock offers the greatest sensitivity. Based on a comparison of the S/N ratios of the peaks in Figures 2B and 2C, an improvement in sensitivity by a factor of 1.25±0.12 has been obtained. The sensitivity gain of the CT-g/s-HMQC over the CT-HMQC is relatively uniform for methine sites and this is achieved by the PEP/COS-CT approach. A sensitivity gain of a factor of 1.33±0.20, for the peaks in Figures 2A and 2C, comes from the better relaxation properties of multiple-quantum coherence when compared with single-quantum coherence. This sensitivity gain was not uniform, and no sensitivity gain was obtained for some peaks. The reasons for this are that spin lock cannot prevent the leakage of magnetization from H_α to H_β if they have almost the same chemical shifts, and the ^{1}H-^{1}H dipole-dipole interaction discussed above.

Figures 3A–B are 2D slices taken from the 3D constant time g/s-NOESY-HMQC spectrum and its HSQC counterpart, and Figures 3C–D are 2D slices taken from the 3D doubly sensitivity enhanced TOCSY-HMQC spectrum and its corresponding HSQC spectrum, respectively. All spectra are measured at 23 °C and all 2D slices are taken at a $^{13}C_\alpha$ shift of 65.1 ppm. These spectra clearly show that the 3D CT-g/s-NOESY-HMQC and the doubly sensitivity enhanced TOCSY-HMQC experiments have much better sensitivity than their HSQC counterparts. It should be pointed out that in these kinds of experiments, the spectra are not symmetrical about the diagonal, and

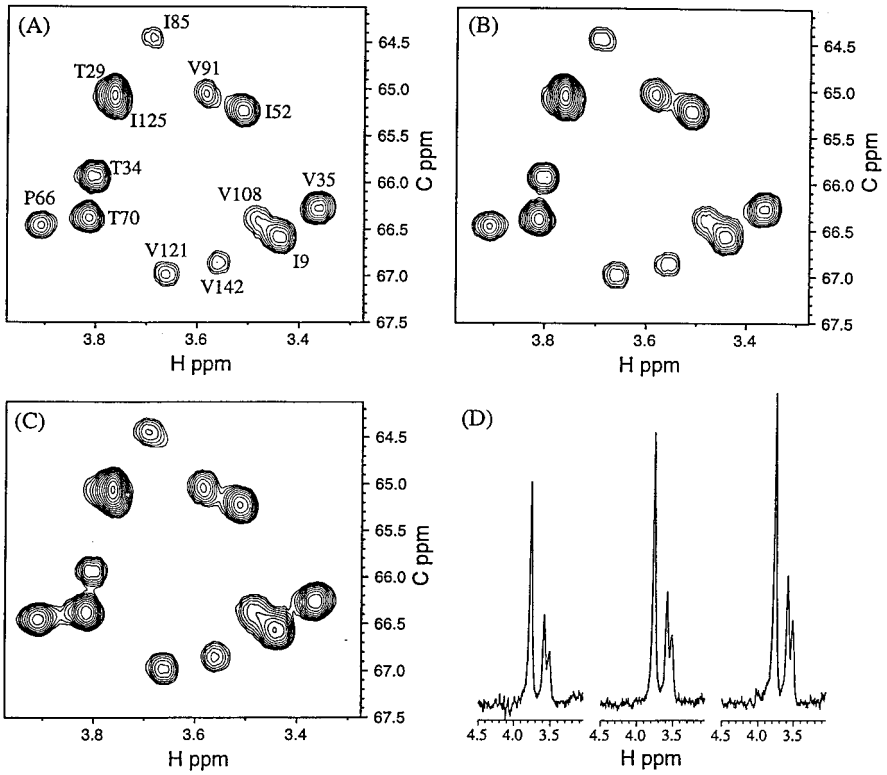

Figure 2. Small regions of spectra of the apo-form of calmodulin recorded at 27 °C in D_2O with (A) the 2D CT-g/s-HSQC experiment, (B) the 2D CT-HMQC experiment (Grzesiek and Bax, 1995), and (C) the proposed 2D CT-g/s-HMQC experiment. (D) 1D cross-sections from A–C, taken at a ^{13}C shift of 65.1 ppm (A, left; C, right). The sizes of the 2D FIDs recorded were $90^* \times 1024^*$ with '*' denoting complex data. These spectra were obtained by Fourier transformation with the same experimental and data processing parameters and have been scaled to the same noise level with the contour levels being spaced by a factor of 1.2. Linear prediction was not used, and data processing was carried out by using the NMRPipe software package (Delaglio et al., 1995).

the peaks (H_α, H_β) and (H_β, H_α) experience different magnetization pathways and relaxation processes. The magnetization transfer of the peaks with sensitivity enhancement is $H_{\beta,\gamma,\ldots} \rightarrow H_\alpha \rightarrow C_\alpha \rightarrow H_\alpha$. Therefore, in the ^{13}C separated NOESY and TOCSY spectra, the sensitivity enhanced peaks are located within the F1 (aliphatic proton) and F3 (H_α proton) regions.

Although the demonstrations of our experiments were performed on a D_2O sample, a sample in H_2O could also be used. In such a case, the gradient used to select the magnetization pathway can also be used to suppress the water signal. Water presaturation should be avoided because it will destroy signals under and near the water resonance. Instead, a strong gradient should be used to achieve good water signal suppression. However, the greater presence of amide protons in an H_2O sample would increase the homonuclear dipole-dipole interaction induced relaxation, thus reducing the sensitivity gain of CT-g/s-HMQC over its HSQC and CT-HMQC counterparts. We have also performed the CT-g/s-HMQC experiment in H_2O. This experiment showed that good suppression of the water signal could be achieved and a sensitivity enhancement could be obtained, though it was less than that when performing the experiment in D_2O (data not shown).

Conclusions

In summary, we have proposed a constant time, gradient and sensitivity enhanced HMQC experiment (CT-g/s-HMQC) with a spin lock during the t_1 evolution period to eliminate homonuclear coupling effects. A significant sensitivity improvement over both its HSQC counterpart and the conventional HMQC experiment was obtained. This experiment will be particularly useful for the NMR study of ^{13}C labeled proteins of moderate sizes when the protein is at the slow tumbling limit. The existence of ^1H-^1H dipole-

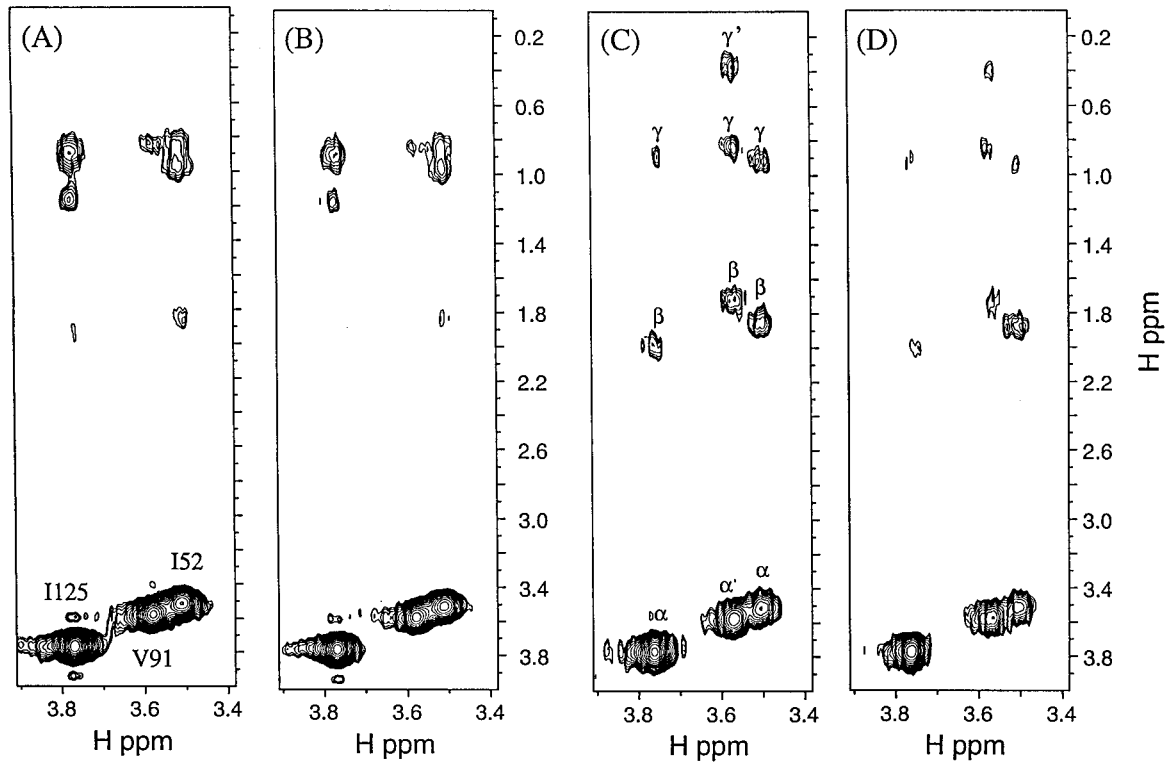

Figure 3. 2D slices (F1/F3) of ^{13}C separated NOESY spectra recorded at 23 °C from (A) the CT-g/s-NOESY-HMQC experiment, (B) the CT-g/s-NOESY-HSQC experiment, and ^{13}C separated TOCSY spectra from (C) doubly sensitivity enhanced TOCSY-HMQC, and (D) doubly sensitivity enhanced TOCSY-HSQC experiments. All 2D slices are at a ^{13}C shift of 65.1 ppm. All experimental and processing parameters are the same for corresponding experiments and the Fourier transform spectra are plotted at the same noise level. The NOESY mixing time is 80 ms. The TOCSY mixing time is 40 ms with a power of 3.2 kHz. The sizes of the 3D NOESY and TOCSY FID matrices are $76^* \times 36^* \times 1024^*$ and $64^* \times 32^* \times 1024^*$, respectively. The contours are spaced by a factor of 1.2.

dipole interactions reduces the advantage of the CT-g/s-HMQC experiment. However, random fractional deuteration of proteins can reduce this effect, and the CT-g/s-HMQC experiment could be applied to larger proteins if they are partially deuterated. This experiment is also well suited to NMR studies of nucleic acids, where many of the ^{13}C attached protons are of the methine type, and the scarcity of ^{1}H-^{1}H dipolar interactions means that ^{13}C-^{1}H dipolar interaction will be the dominant relaxation mechanism.

We have also extended the basic CT-g/s-HMQC sequence to 3D NOESY-HMQC and doubly sensitivity enhanced TOCSY-HMQC experiments. The resulting spectra show a clear sensitivity enhancement over their HSQC counterparts. These experiments demonstrate that the CT-g/s-HMQC pulse sequence can be applied to many other kinds of 3D experiments to facilitate NMR studies of proteins and nucleic acids of moderate size.

Acknowledgements

The authors thank Dr. David Smith for helpful discussions, Dr. Mingjie Zhang for allowing us to use his ^{13}C and ^{15}N labeled calmodulin sample and Dr. Ad Bax for the assignments of calmodulin. This work was supported by grants from the Research Grant Council of Hong Kong (HKUST 6038/98M and 6197/97M) and the Hong Kong Biotechnology Research Institute is acknowledged for the purchase of the spectrometer.

References

Cavanagh, J. and Rance, M. (1993) *Annu. Rep. NMR Spectrosc.*, **27**, 1–58.

Delaglio, F., Grzesiek, S., Vuister, G., Zhu, G., Pfeifer, J. and Bax, A. (1995) *J. Biomol. NMR*, **6**, 277–293.

Ernst, R.R., Bodenhausen, G. and Wokaun, A. (1987) *Principles of Nuclear Magnetic Resonance in One and Two Dimensions*, Clarendon Press, Oxford.

Griffey, R.H. and Redfield, A.G. (1987) *Quart. Rev. Biophys.*, **19**, 51–82.
Grzesiek, S., Kuboniwa, H., Hinck, A.P. and Bax, A. (1995) *J. Am. Chem. Soc.*, **117**, 5312–5315.
Grzesiek, S. and Bax, A. (1995) *J. Biomol. NMR*, **6**, 335–339.
Hyre, D.E. and Spicer, L.D. (1995) *J. Magn. Reson.*, **B108**, 12–21.
Ikura, M., Kay, L.E., Krinks, M. and Bax. A. (1991) *Biochemistry*, **30**, 5498–5504.
Kay, L.E., Keifer, P. and Saarinen, T. (1992) *J. Am. Chem. Soc.*, **114**, 10663–10665.
Levitt, M.H. (1997) *J. Magn. Reson.*, **126**, 164–182.
Marino, J.P., Diener, J.L., Moore, P.B. and Griesinger, C. (1997) *J. Am. Chem. Soc.*, **119**, 7361–7366.
Muhandiram, D.R. and Kay, L.E. (1994) *J. Magn. Reson.*, **B103**, 203–216.
Nietlispach, D., Clower, R., Broadhurst, T.R., Ito, W.Y., Keeler, J., Kelly, M., Ashurst, J., Oschkinat, H.P., Domaille, J. and Laue, E.D. (1996) *J. Am. Chem. Soc.*, **118**, 407–415.
Palmer, A.G., Cavanagh, J., Wright, P.E. and Rance, M. (1991) *J. Magn. Reson.*, **93**, 151–170.
Palmer, A.G., Skelton, N.J., Chazin, W.J., Wright, P.E. and Rance, M. (1992) *Mol. Phys.*, **75**, 699–711.
Patt, S.L. (1992) *J. Magn. Reson.*, **96**, 94–102.
Reisman, J., Jariel-Encontre, I., Hsu, V.L., Parell, J., Geiduschek, E.P. and Kearns, D.R. (1991) *J. Am. Chem. Soc.*, **113**, 2787–2789.
Sattler, M., Schwendinger, M.G., Schleucher, J. and Griesinger, C. (1995) *J. Biomol. NMR*, **5**, 11–22.
Schleucher, J., Sattler, M. and Griesinger, C. (1993) *Angew. Chem. Int. Ed. Engl.*, **32**, 1489–1491.
Schleucher, J., Schwendinger, M., Sattler, M., Schmidt, P., Schedletzky, O., Glaser, S.J., Sørensen, O.W. and Griesinger, C. (1994) *J. Biomol. NMR*, **4**, 301–306.
Shaka, A.J., Lee, C.J. and Pines, A. (1988) *J. Magn. Reson.*, **77**, 274.
Shang, Z., Swapna, G.V.T., Rios, C.B. and Montelione, G.T. (1997) *J. Am. Chem. Soc.*, **119**, 9274–9278.
Sørensen, O.W., Eich, G.W., Levitt, M.H., Bodenhausen, G. and Ernst, R.R. (1983) *Prog. NMR Spectrosc.*, **16**, 163–192.
Swapna, G.V.T., Rios, C.B., Shang, Z. and Montelione, G.T. (1997) *J. Biomol. NMR*, **9**, 105–110.
Tjandra, N., Kuboniwa, H., Ren, H. and Bax, A. (1995) *Eur. J. Biochem.*, **230**, 1014–1024.
Torchia, D.A., Sparks, S.W. and Bax, A. (1988) *J. Am. Chem. Soc.*, **110**, 2320–2321.
Wijmenga, S.S., van Mierlo, P.M. and Steensma, E. (1996) *J. Biomol. NMR*, **8**, 319–330.
Yamazaki, T., Lee, W., Arrowsmith, C.H., Muhandiram, D.R. and Kay, L.E. (1994) *J. Am. Chem. Soc.*, **116**, 11655–11666.
Zhu, G., Live, D. and Bax, A. (1994) *J. Am. Chem. Soc.*, **116**, 8370–8371.
Zhu, G., Kong, X.M. and Sze, K.H. (1998) *J. Magn. Reson.*, **135**, 232–235.